Journal of Solid Mechanics Vol. 13, No. 2 (2021) pp. 134-143
DOI: 10.22034/jsm.2020.1889852.1537

Comparative Analysis of Energy Absorption Capacity of Single and Nested Metal Matrix Composite Tubes Under Quasi-Static Lateral and Axial Loading

S. Dehghanpour [1], K. Hosseini Safari [2, *], F. Barati [3], M.M. Attar [3]

[1] *Department of Mechanics, Tuyserkan Branch, Islamic Azad University, Tuyserkan, Iran*
[2] *Department of Mechanical Engineering, Central Tehran Branch, Islamic Azad University, Tehran, Iran*
[3] *Department of Mechanical Engineering, Hamedan Branch, Islamic Azad University, Hamedan, Iran*

Received 14 February 2021; accepted 2 April 2021

ABSTRACT

In this paper the behavior of nested tube systems under quasi-static compressive loading is investigated. Two nested tube systems with metal matrix composite are subjected to compressive loads so that in the system A the exterior and interior tubes are under axial and lateral loads, respectively but in the system B the exterior and interior tubes are under lateral and axial loads, respectively. Furthermore, these systems behavior are studied numerically. The results show that energy absorption capacity for both of nested tube systems is greater than the sum of energy absorption capacities of two constitutive tubes when loaded individually. Also, it is shown that the absorbed energy for system A is greater than that of system B. In this research the effects of section geometry and the condition of loading (axial or lateral)of thin-walled tubes on energy absorption capacity and the value of the peak load are studied both experimentally and numerically.

Keywords: Nested tube systems tubes; Energy absorption; Metal matrix composite; Quasi-static loading.

1 INTRODUCTION

DUE to simple process of fabrication, thin walled tubes are used in modem vehicle structures as energy absorber. These tubes dissipate the impact energy in the form of folding and plastic deformation. Among these tubes, the circular sections are mostly used. Metallic tubes can dissipate energy in the forms of axial and lateral crushing which are demonstrated briefly in the following parts.

1.1 Axial crushing

This type of deformation occurs during axial compressive loading and has a great capacity of energy absorption, because most of the tube material participates in plastic deformation and energy dissipation processes. Alexander [1] presented

[*] Corresponding author. Tel.: +98 9123869204.
E-mail address: keivan.hosseini.safari@gmail.com (K. Hosseini Safari)

the first analysis about the collapse of cylindrical tubes under axial load in order to obtain relationships for design of nuclear fuel containers. Pugsley and Macaulay [2] studied the symmetric and asymmetric axial crushing of cylindrical tubes analytically. Pugsley [3] introduced two dimensionless parameters named effectiveness and solidity ratio Io compare analytical results and experimental data about thin walled structures. Mamalis and Johnson [4] showed that tubes with ratios of radius/thickness smaller than 4o-45 exhibit symmetric Progressive buckling whereas for greater ratios the mode of collapse is asymmetric. They also showed that transformation from symmetric to asymmetric mode may occur during test. Abramowicz [5] defined an effective crushing distance for collapse of thin walled tubes under axial folding. He studied the effect of strain rate sensitivity on the axial dynamic crushing of a cylindrical tube. Abramowicz et al. [7] derived a theoretical formula for the effective crushing distance and showed that this relation is in good agreement with the static and dynamic crushing of mild steel tubes. Mamalis et al. [8] showed that circular grooves on the outer surface of tubes reduce the first peak load of buckling. Bardi et al. [9] studied the axial crushin8 of extruded tubes and compared their experimental values for average crushing force with theoretical results of Alexander and Wierzbicki. Sedghi et al. [10] investigated the effects of circumferential grooves on the axial crushing and energy absorption of cylindrical tubes and showed that the fold wave length and efficiency of the system are independent of the geometry of the grooves section. Kheirkhah et al. [11] showed that the section geometry has considerable effect on the energy absorption. The circular composite tube has the most energy absorption capacity and the most average force among all investigated sections. Rihuan et al. [12] concluded that the shorter tailor rolled tubes and proper length of thickness transition zone is of more benefit to improve energy absorption efficiency. It can be concluded that the optimization thickness distribution and material strength of tailor rolled tubes can be designed according to the actual multi-requirements, and can be large-lot manufactured by variable gauge rolling technology to maximize the energy absorption and material saving. Zhang et al. [13] found the optimal design of the 2nd order HCT, multi-objective optimization is performed by employing radial basis function (RBF) neural networks and multi-objective particle swarm optimization (MOPSO) algorithm. The several optimal structures are obtained under different peak crushing force (PCF). The findings of this research offer a new route of designing novel crashworthiness structure with high energy absorption capacity.

1.2 Lateral loading

In this type of deformation which occurs due to lateral compression, the plastic hinges are formed parallel to the axis of the tube. Deformations in this mode are more extensive relative to the lateral indentation. Although these deformations are not as large as axial crushing, are studied here due to their application in some vehicles as energy absorber in lateral impacts. Mutchler [14] studied numerically in-plane loading and energy absorption of aluminum tubes which were constrained between two rigid plates. Deruntz and Hodge [15] investigated the behavior of tubes using finite element method and assumed that the deformed contour consists of four circular arcs which maintain their original radius and plastic deformation occurs in the hinges only. Reid and Reddy [16] studied compression of tubes with lateral constraints and investigated the effect of these constraints theoretically. They [17] carried out experiments on thin-walled structures with a circular section and different lengths and studied the effect of lengths on the energy absorption capacity. Gupta et al. [18] studied also the in-plane loading of thin-walled structures with circular section and proposed an analytical model for prediction of deformations of tubes and compared them with experimental data. Morris et al. [19] investigated lateral compression of nested systems and showed that increasing number of tubes results in the increase of absorbed energy; furthermore, this property is affected by the vertical and oblique constraints. Laterally loaded tubes have a distinct advantage over tubes compressed axially due to fact that the bending collapse mode generated from lateral loading result in a smooth force-deflection response. Also, the laterally loaded tubes do not undergo any kind of unstable deformation mode even under the off-axis loading. However, the deformation mode of these structures is plastic bending at plastic hinges. Dehghanpour et al. [20] investigated from the surveys is indicates that in a same condition which mentioned above, samples with square cross section, absorb more energy compare to rectangular cross section, and also by increscent in speed of loading, energy absorption would be more. This deformation mode results in plastic strains localization around the plastic hinges and makes the dissipation of energy through the lateral collapse inefficient. Therefore, to overcome the aforementioned drawback and to enhance the energy absorbing capacity of single empty tubes, foam-filled components [21–23] and nested tube systems have [24–27] been proposed. Dehghanpour et al. [28] studied is to survey the deformation and energy absorption of tubes with different type of cross section (rectangular, circle, square, hexagonal) and with similar volumes, height, mean cross section, and material under three different loading with different indenter. Lateral loading of tubes are quasi-static type and beside as numerical analysis, also experimental experiences has been performed to evaluate the accuracy of the results. Results from the surveys is indicates that in a same condition

which mentioned above, samples with square cross section, absorb more energy compare to another cross section. Baroutaji et al. [29] studied the responses of nested tubes systems under quasi-static and dynamic lateral loading and survey the effect of geometrical and loading parameters and determined the best nested tubes system. In this paper, the results of experimental and numerical studies on the behavior of two different. Systems of nested tubes are presented. In the first system, system A, the exterior and interior tubes are subjected to axial and lateral load, respectively and in the second system, system B, the role of tubes is reversed. This research shows that the energy absorption capacity of the nested tube systems is greater than the sum of dissipated energies by the constitutive tubes when are loaded individually. Furthermore, it is shown that system A is more effective than system B. In this study, since the tubes are designed to be exposed to axial and lateral loads, it can protect the system against impacts that protect the axial and lateral.

2 EXPERIMENTS

2.1 Samples specifications

Since there were not available the tubes with predefined dimensions, they were made manually. In this procedure, due to welding process effects, may there be some unwanted changes in properties which are diminished by slowly cooling and grinding of weld line. The above metallic matrix composite plates were made of aluminum and carbon fibers by the device shown in Fig. 1. plate with a thickness of 1.5 *mm* was used to make the specimens. Tension test: In order to determine mechanical properties of plate, tension test based on ASTM 8M-98 is carried out using INSTRON 8305 apparatus. Results of this test are presented in Table1. Based on data presented in Table 1, Mechanical properties of metal matrix composite material are shown.

Fig.1
Device for made mmc.

Table 1
Mechanical properties of metal matrix composite material.

Parameters	E_f [*GPa*]	E_m [*GPa*]
Value	250, 200, 80	80, 4.2

Chemical compositions: In order to determine material compositions of the plate three 3×3 *cm* specimens were tested and the results are listed in Table 2. Comparing these data with standard hand books verifies that the material of the plate is AL3003-H12.

Table 2
Chemical compositions of the specimens' material.

Chemical	Percentage
Al	97.81
Si	0.38
Zn	0.047
Mn	1.06
Sn	0.00017
Fe	0.55
Cu	0.15
Sum	99.99717

Samples dimensions All of the samples are cylinders with the same material and have a thickness of 1.5 *mm*. Tubes are designed so that one tube is fitted in the other with axes perpendicular to each other. The sample dimensions are presented in Table 3.

Table 3
Dimensions of the specimens.

	Exterior tube	Interior tube
Diameter (*mm*)	100	60
Length (*mm*)	64	72
Thickness (*mm*)	1.5	1.5

Coding the specimens for the system A, the exterior tube is subjected to axial load whereas the interior tube is set in it so that undergoes lateral load. For the system B, the tube with the greater diameter is subjected to lateral load and the inner tube undergoes axial load. In both of the systems, axes of the inner and the outer tube are perpendicular to each other. Fig. 2 shows the configurations of these systems. Mechanical and geometrical properties of the tubes for both of the systems are the same (as presented in Tables 1 and 3). The codes which are assigned to the tubes are presented in Table 4.

Table 4
Samples codes in systems A and B.

Specimen shape	Code	
	System A	System B
Exterior tube	CB_{out}	CB_{in}
Interior tube	CS_{in}	CS_{out}
Nested tube systems	$N_A B_{out} S_{in}$	$N_B B_{in} S_{out}$

(a) (b)

Fig.2
Tubes configuration a: System A , b: System B.

2.2 Quasi-static tests

Test procedure: Quasi-static compression tests are carried out using Instron 8305 apparatus (Fig. 3). This machine has two jaws the upper of which is stationary and the lower one can move with a predefined velocity in a specific distance. The load is exerted by hydraulic system. The specimen is set between jaws and the load-displacement curve is plotted during deformation. The rate of loading for all tests is 100 *mm/s*. At first, each of tubes is loaded individually and then the nested tube systems is subjected to compression until the maximum displacement is achieved. The load-displacement curve for each test is plotted and the absorbed energy equal to the area under the curve is calculated. In this manner, it is possible to compare the efficiency of the nested tube systems with the individual tubes. In order to increase accuracy of the answers for each case, three tests with the same conditions are done.

Fig.3
Instron 8305 apparatus.

3 NUMERICAL SIMULATIONS

Since the experimental studies involve much expenses and difficulties, and the analytical theories about plastic deformations are complex, the researchers' tendency is toward using numerical soft wares. LS-DYNA software due to its capabilities in modeling impact loads and high deformation processes has an extensive application in this field. In this research, besides the experimental tests, the numerical simulation is done using LS-DYNA 970. Three dimensional simulations are carried out for modeling the loading of the nested tube systems A and B and their parts. Tubes dimensions are the same as tested specimens (as listed in Table 3). The upper surface is stationary and the lower one is moved toward it with a velocity of 100 *mm/s*. The boundary conditions are like those in tests. Material behavior is modeled using mat- piecewise linear plasticity and the material properties are taken from tension test. Proper contacts between the tube elements and the end plates, and between the tube elements with each other are defined.

4 RESULTS

4.1.1 Test results related to the system A

Axial loading of the exterior tube the exterior tube is subjected to axial compression and its load-displacement curve is plotted. This curve associated with the tube shape at the beginning and end of loading process is shown in Fig. 4(a). The value of absorbed energy is calculated from this curve. Lateral loading of the interior tube the interior tube is subjected to lateral compression. The load-displacement curve and the tube deformation at the beginning and end of loading process is shown in Fig. 4(b). Loading of the nested tube systems A: This system is loaded so that the outer and the inner tubes undergo axial and lateral loads, respectively. This system configuration before and after loading associated with its load-displacement curve is shown in Fig. 4(c). The peak load, the absorbed energy and the average force for these tests are presented in Table 5.

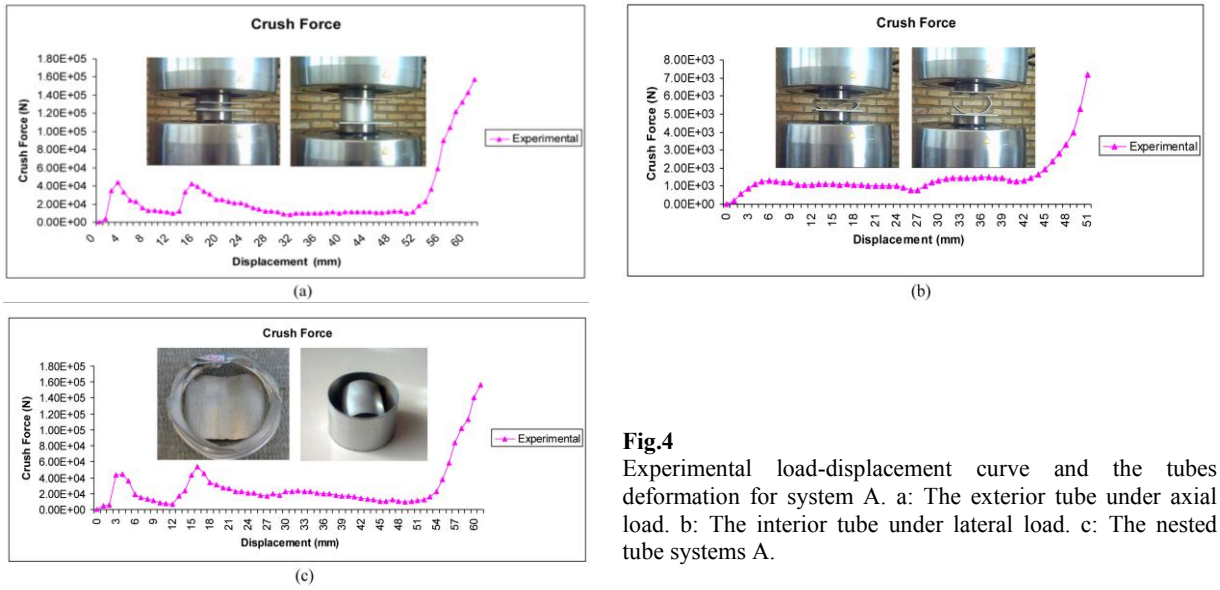

Fig.4
Experimental load-displacement curve and the tubes deformation for system A. a: The exterior tube under axial load. b: The interior tube under lateral load. c: The nested tube systems A.

Table 5
Comparison between the peak load, the average load and the absorbed energy related to the individual tubes and nested tube systems A.

Specimen shape	Code	Crushing Length(*mm*)	Peak load (*N*)	Mean force (*N*)	Absorbed energy (*J*)
Exterior tube subjected to out of plane loading	CB_{out}	52	44000	14134.61	735
Interior tube subjected to in plane loading	CS_{in}	44	1130	1172.72	51.6
Nested tube systems (A)	$N_A B_{out} S_{in}$	52	45000	18846.15	980

4.1.2 Test results related to system B

Lateral loading of the exterior tube: The exterior tube is subjected to lateral compression and its load-displacement curve is plotted. These curves associated with the tube shape at the beginning and end of loading process are shown in Fig. 5(a). Axial loading of the interior tube the interior tube is subjected to axial compression and its load-displacement curve and the tube deformations at the beginning and end of loading process are shown in Fig. 5(b). Loading of the nested tube systems B: This system is loaded so that the outer and the inner tubes are subjected to lateral and axial loads, respectively. This system configuration, before and after loading associated with its load-displacement curve, is shown in Fig. 5(c). The results of tests on the nested tube systems B and its parts are listed and compared in Table 6.

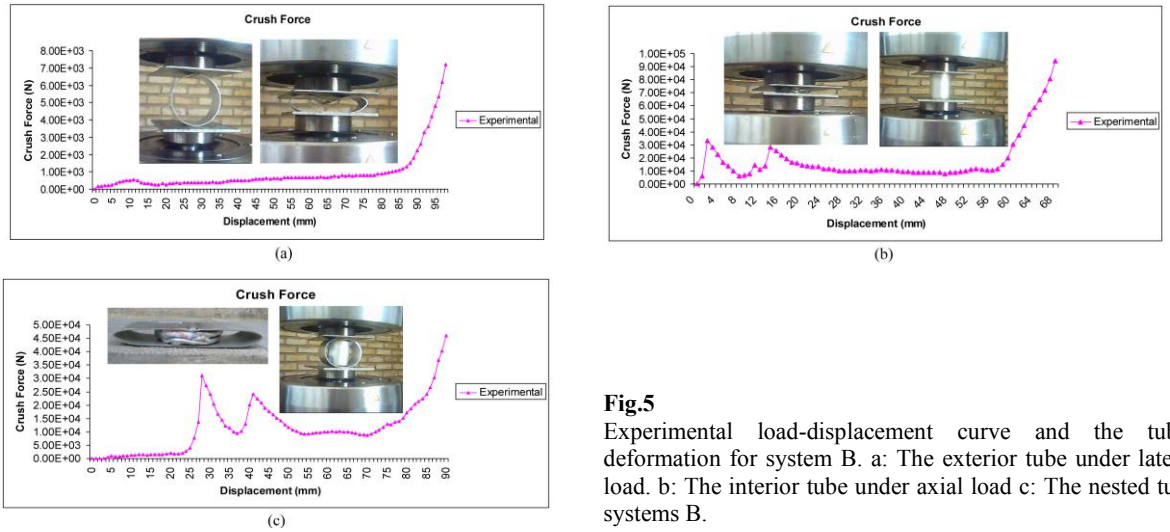

Fig.5
Experimental load-displacement curve and the tubes deformation for system B. a: The exterior tube under lateral load. b: The interior tube under axial load c: The nested tube systems B.

Table 6
Comparison between the peak load, the average load and the absorbed energy related to the individual tubes and nested tube systems B.

Specimen shape	Code	Crushing Length(*mm*)	Peak load (*N*)	Mean force (*N*)	Absorbed energy (*J*)
Exterior tube subjected to in plane loading	CB_{in}	88	450	567.04	49.9
Interior tube subjected to out of plane loading	CS_{out}	57	33300	12245.61	698
Nested tube systems (B)	$N_B B_{in} S_{out}$	84	31000	10297.6	865

4.2.1 Simulations related to system A

Exterior tube: The exterior tube whose dimensions are listed in Table 3 is subjected to axial load. The finite element model of the exterior tube associated with the curves of load- displacement and energy-displacement is shown in Fig. 6(a). Interior tube: The interior tube is subjected to lateral load. The finite element model and the curves of load-displacement and energy-displacement for this tube are shown in Fig. 6(b). The nested tube systems A Compressive loading of system A is simulated as in the test. The finite element model of the system associated with the load-displacement and energy-displacement curves are shown in Fig. 6(c). Also, the results of loading system A and its constitutive tubes are listed in Table 7.

Table 7
Comparison between the peak load, the average load and the absorbed energy of the nested tube systems A and its parts.

Specimen shape	Crushing Length (*mm*)	Peak load (*N*)	Mean force (*N*)	Absorbed energy (*J*)
Exterior tube subjected to out of plane loading	51	40700	13960.78	712
Interior tube subjected to in plane loading	48	1020	1081.25	51.9
Nested tube systems (A)	51	40700	17705.88	903

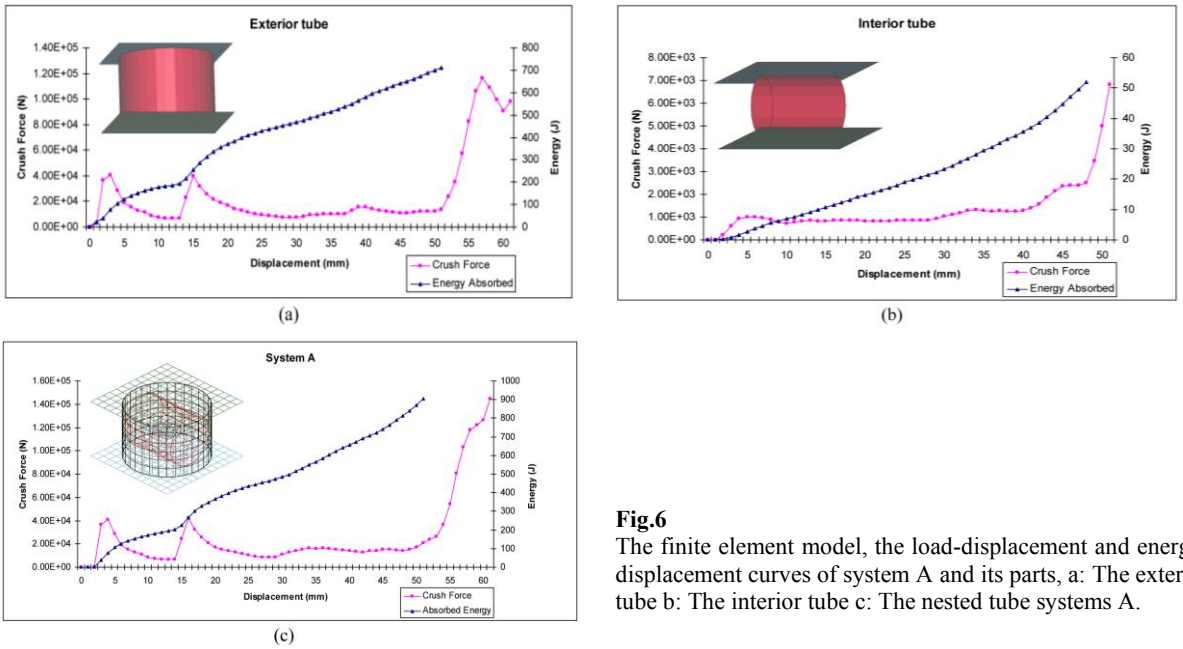

Fig.6
The finite element model, the load-displacement and energy-displacement curves of system A and its parts, a: The exterior tube b: The interior tube c: The nested tube systems A.

4.2.2 Simulations related to system B

Exterior tube: The exterior tube whose dimensions are listed in Table 3 is subjected to lateral load. The finite element model of the tube associated with the curves of load-displacement and energy-displacement are shown in Fig. 7(a). Interior tube: The interior tube is subjected to axial load. The finite element model, the curves of load-displacement and energy-displacement for this tube are shown in Fig. 7(b). The nested tube systems B: Compressive loading of system B is simulated as in the test. The finite element model of the system associated with the load-displacement and energy displacement Curves of this system is shown in Fig. 7(c). Furthermore, the results of simulations of system B and its parts are presented in Table 8.

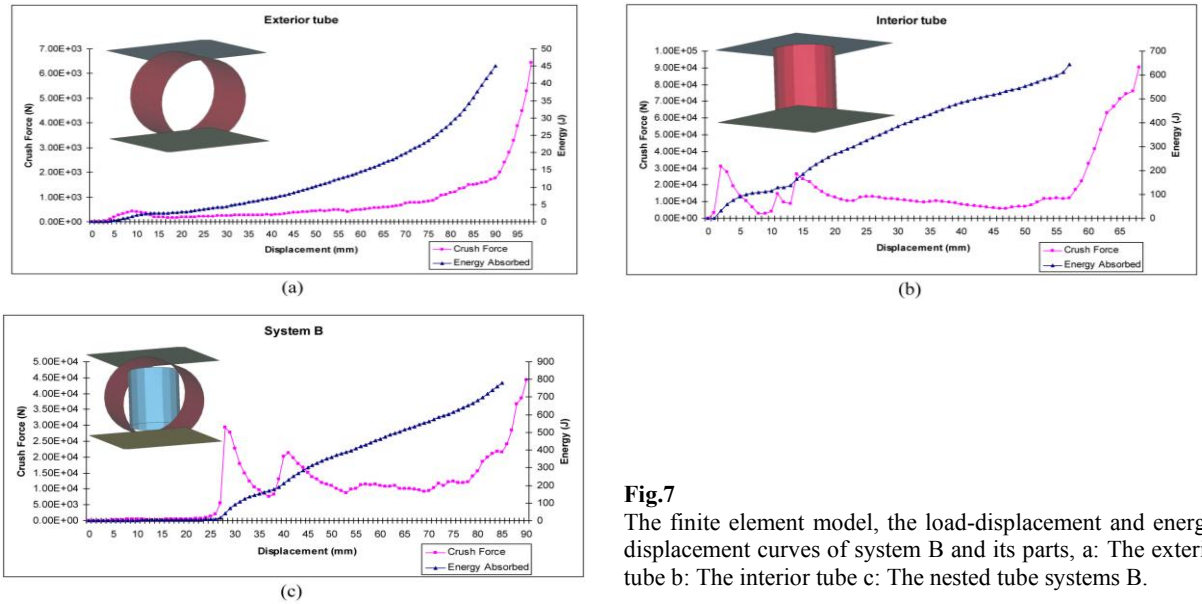

Fig.7
The finite element model, the load-displacement and energy-displacement curves of system B and its parts, a: The exterior tube b: The interior tube c: The nested tube systems B.

Table 8
Comparison between the peak load, the average load and the absorbed energy of the nested tube systems B and its parts.

Specimen shape	Crushing Length(*mm*)	Peak load(*N*)	Mean force(*N*)	Absorbed energy(*J*)
Exterior tube subjected to in plane loading	90	423	501.11	45.1
Interior tube subjected to out of plane loading	57	31100	11315.78	645
Nested tube systems (B)	85	29300	9176.47	780

5 COMPARISON AND DISCUSSION

In this section, the results of the experimental and numerical simulations are compared and the superiority of the nested tube systems with respect to individual tubes is shown.

5.1 The system A

As shown in Table 9, the sum of energies absorbed by two parts of system A when are loaded individually is equal to 786.6*J* which is less than 980*J*, the absorbed energy by the nested tube systems. The load-displacement curves of the exterior tube, the interior tube and the nested tube system A from tests and simulations are plotted and compared in Fig. 8.

Table 9
Comparison between the numerical and experimental values of the absorbed energy for the system A.

Specimen shape	Code	Absorbed energy(*N.m*) (Numerical)	Absorbed energy(*N.m*) (Experimental)	Difference (%)
Exterior tube subjected out of plane loading	CB_{out}	712	735	3.12
Interior tube subjected in plane loading	CS_{in}	51.9	51.6	-0.58
Nested tube systems (A)	$N_A B_{out} S_{in}$	903	980	7.58

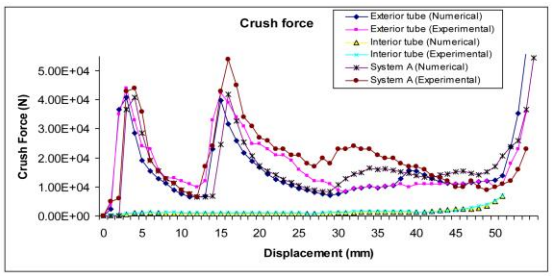

Fig.8
Comparison between the experimental and numerical load-displacement curves for the exterior tube under axial load, the interior tube under lateral load and the nested tube systems A.

Since the exterior tube is subjected to axial load and undergoes more deformations with respect to interior tube under lateral load, its energy absorption capacity is greater. For the nested tube systems A, due to additional constraints and interaction between tubes, the absorbed energy is greater than the sum of values of this parameter for individual parts. Fig.8 shows that the first peak loads for the exterior tube and the nested tube systems are nearly the same. This is true because in both cas the exterior tube is subjected to axial load at first. Continuing the loading process results in more deformations and the interaction between the inner and outer tube needs greater loads. Therefore, the average crushing force for the nested tube systems is larger than that of the exterior tube.

5.2 The system B

As shown in Table 10 the sum of the absorbed energies by two parts of system B when loaded individually is equal to 747.9*J* which is less than 865J, the absorbed energy by the nested tube systems, which indicates the more efficiency of the nested tube systems.

Table 10
Comparison between the numerical and experimental values of the absorbed energy for system B.

Specimen shape	Code	Absorbed energy(*J*) (Numerical)	Absorbed energy(*J*) (Experimental)	Difference (%)
Exterior tube subjected to in plane loading	CB_{in}	45.1	49.9	9.61
Interior tube subjected to out of plane loading	CS_{out}	645	698	7.59
Nested tube systems (B)	$N_B B_{in} S_{out}$	780	865	9.82

The load-displacement curves for the exterior tube, interior tube and the nested tube systems B from tests and numerical simulations are compared in Fig. 9. It is clear from this figure that before contact and interaction between tubes, the load is approximately constant and when the interior tube begins to deform plastically, the force increases suddenly and this is the cause of increase in capacity of energy absorption for the nested tube systems.

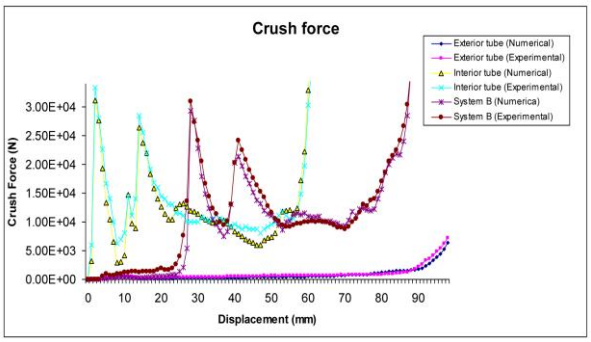

Fig.9
Comparison between the experimental and numerical load-displacement curves for the exterior tube under lateral load, the interior tube under axial load and the nested tube systems B.

6 CONCLUSIONS

Comparing the values of absorbed energies in Tables 9 and 10 reveals that system A is more efficient than system B. When the tubes are loaded laterally, increasing the diameter/thickness ratio reduces the energy absorption capacity. The exterior tube of system B and the interior tube of system A are subjected to lateral loads since the diameter/thickness ratio of the former is greater than that of the later, its ener8y absorption capacity is smaller. Besides, between the exterior tube of system A and the interior tube of system B which are subjected to the axial load, the former absorbs greater energy due to its greater mass and plastic deformations. Therefore, the total energy absorbed by system A is greater than that of system B.Comparison between the energy absorption capacity of two systems and their parts is shown in Fig.10.

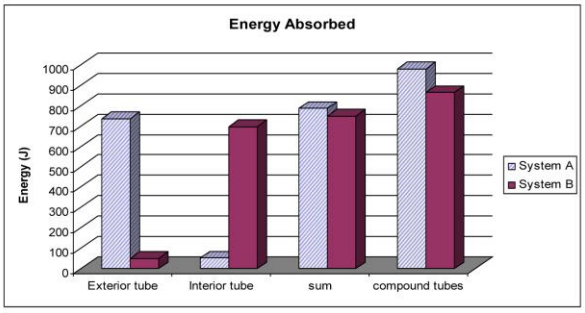

Fig.10
Comparison between the energy absorption capacity of systems A and B.

In this paper the energy absorption capacity of two nested systems and their parts under compression load are investigated both experimentally and numerically. The important results of this research are as follow:The absorbed energy of the nested tube systems A is 24% greater than the sum of energies absorbed by its parts when loaded individually; this value for system B is 15%.The energy absorption capacity of system A is about 13% greater than that of system B.

REFERENCES

[1] Alexander J. M., 1960, An approximate analysis of the collapse of thin cylindrical shells under axial loading, *Journal of Mechanics and Applied Mathematics* **13**(1): 10-15.

[2] Pugsley Sir A., Macaulay M.,1960, The large scale crumpling of thin cylindrical columns, *Journal of Mechanics and Applied Mathematics* **13**: 1-9.

[3] Pussley Sir A.,1960, The crumpling of tubular structures under impact conditions, *Proceedings of the Symposium on The Use of Aluminum in Railway Rolling Stock Institute of Locomotive Engineers, The Aluminum Development Association*, London.

[4] Mamalis A. G., Johnson W.,1983, The Quasi-static crumpling of thin-walled circular and frusta under axial compression, *International Journal of Mechanical Sciences* **25**(9/10): 713-732.

[5] Abramowicz W.,1983, The effective crushing distance in axially compressed thin walled metal columns, *International Journal of Impact Engineering* **1**(3): 309-317.

[6] Abramowicz W., Jones N.,1984, Dynamic axial crushing of circular tubes, *International Journal of Impact Engineering* **2**(3): 263-281.

[7] Abramowicz W., Jones N.,1986, Dynamic progressive buckling of circular and square tubes, *International Journal of Impact Engineering* **4**(4): 243-270.

[8] Mamalis A. G., Manolakos D.E., Saigal S., Viegelahn G., Johnson W., 1986, Extensible plastic collapse of thin-walled frusta as energy absorber, *International Journal of Mechanical Sciences* **28**(4): 219-229.

[9] Bardi F. C., Yun H.D., Kyriakides S.,2003, On the axisymmetric progressive crushing of circular tubes under axial compression, *International Journal of Solids and Structures* **40**: 3137-3155.

[10] Sedghi M., Alavi Nia A., Labbafi H., Atmri P.,2008, Effect of circumferential gFooves geometries on crashworthiness of ax axially loaded cylindrical tubes, *16th Annual and 12th International Conference Mechanical Engineering*, Bahonar University, Kerman, Iran.

[11] Kheirikhah M.M , Dehghanpour S. , Rahmani M.,2016, Quasi-static axial compression of thin-walled circular composite tubes, *Journal of Structural Engineering and Geo-Techniques* **6**(1): 9-13.

[12] Rihuan L.,Xianghua L.,Shoudong C.,Xianlei H.,Lizhong L., 2017, Axial crashing analysis for tailor rolled square tubes with axially graded both wall thickness and material strength,*Thin-Walled Structures* **117**: 10-24.

[13] ZhangY.,Xu X.,Wang J.,Chen T.,Wang C.H.,2018, Crushing analysis for novel bio-inspired hierarchical circular structures subjected to axial load, *International Journal of Mechanical Sciences* **140**: 407-431.

[14] Mutchler L. D.,1960, Energy absorption of aluminum tubes, *Journal of Applied Mechanics* **27**(4): 740- 743.

[15] Deruntz V. A. , Hodge P.G., 1963,Crushing of a tube between rigid plates, *Journal of Applied Mechanics* **30**: 391-398.

[16] Reid S. R., Reddy T.Y.,1978, Effects of strain hardening on the lateral compression of tube between rigid plates, *International Journal of Solids and Structures* **14**(3): 213-225.

[17] Reddy T. Y., Reid S.r.,1979, Lateral compression of tubes and tube-system with side constrains, *International Journal of Mechanical Sciences* **21**(3): 187-199.

[18] Gupta N. K., Sekhon G.S., Gupta P.K., 2005, Study of lateral compression of round metallic tube, *Thin-Walled Structures* **43**: 895-922.

[19] Morris E., Olabi A.G., Hashmi M.J., 2005, Analysis of nested tubes type energy absoMrs with different indenters and exterior constraints, *Thin-Walled Structures* **44**: 827-885.

[20] Dehghanpour S., Yousefi A., 2012, Lateral crushing of square and rectangular metallic tubes under different quasi-static conditions, *World Academy of Science, Engineering and Technology, International Journal of Mechanical, Aerospace, Industrial, Mechatronic and Manufacturing Engineering* **6**(1): 628-632.

[21] Fan Z., 2013, Dynamic lateral crushing of empty and sandwich tubes, *International Journal of Impact Engineering* **53**: 3-16.

[22] Baroutaji A.,2015, Analysis and optimization of sandwich tubes energy absorbers under lateral loading, *International Journal of Impact Engineering* **82**: 74-88.

[23] Baroutaji A., Olabi A.G,2014, Lateral collapse of short length sandwich tubes compressed by different indenters and exposed to external constraints, *Materialwissenschaft Werkstofftechnik* **45**(5): 371-384.

[24] Morris E., Olabi A., Hashmi M., 2007, Lateral crushing of circular and non-circular tube systems under quasi-static conditions, *Journal of Materials Processing Technology* **191**(1): 132-135.

[25] Olabi A.,Morris E.,Hashmi S.,Gilchrist M., 2008, Optimised design of nested oblong tube energy absorbers under lateral impact loading, *International Journal of Impact Engineering* **35**(1): 10-26.

[26] Olabi A.,Morris E.,Hashmi S.,Gilchrist M., 2008,Optimised design of nested circular tube energy absorbers under lateral impact loading, *International Journal of Mechanical Sciences* **50**(1): 104-116.

[27] Haibo W., Jialing Y., Hua L., Yuxin S., T.X. Yu., 2015, Internally nested circular tube system subjected to lateral impact loading,*Thin-Walled Structures* **91**: 72-81.

[28] Dehghanpour S. , Khalili H. , Hoseini-Safari K. , Mohammad Y., 2015, Experimental and numerical investigation of lateral loading of thin–walled tube with different indenter, *Journal of Simulation and Analysis of Novel Technologies in Mechanical Engineering* **8**(3): 173-184.

[29] Baroutaji A., Gilchrist M.D. , Olabi A.G., 2016, Quasi-static impact and energy absorption of internally nested tubes subjected to lateral loading, *Thin-Walled Structures* **98**: 337-350.